

## ANATOMICAL INVESTIGATION OF THERMALLY COMPRESSED WOOD PANELS

Dilek Dogu,<sup>a</sup> \* Kamile Tirak,<sup>b</sup> Zeki Candan,<sup>c</sup> and Oner Unsal<sup>c</sup>

Effects of temperature and press pressure on the anatomical structure of solid-wood panels produced by using *Pinus sylvestris* L. (Scotch pine) wood were evaluated. Solid wood panels with dimensions of 250 by 500 by 18 mm were hot-pressed using a laboratory hot press at a temperature of either 120°C or 150°C and pressure of either 5 or 7 MPa for 1 h. Microscopic investigations conducted by Light Microscopy (LM) and Scanning Electron Microscopy (SEM) showed that the highest deformation occurred in earlywood regions of all growth rings for each process condition and the distribution of deformation was not uniform in growth rings. Cell-wall thickness was observed to be an important factor in wood behavior during thermal compressing processes. The results showed clearly that the impact of pressure in wood structure is promoted by increased temperature. Significant densification was observed at the maximum temperature and maximum pressure condition employed in the study, and almost all earlywood layers showed cell collapse. The study revealed that a homogenous structure of growth rings with the uniform earlywood and latewood widths throughout the wood samples plays a major role in prevention of cell collapse. The results indicated that both process conditions and anatomical structure of the wood have an interaction.

*Keywords:* Thermal modification; Thermal compression; Anatomical structure; Cellular failures; Scotch pine

*Contact information:* a: Department of Forest Biology and Wood Protection Technology, Forestry Faculty, Istanbul University, Bahcekoy, Sariyer, 34473, Istanbul, Turkey; b: Department of Forest Biology and Wood Protection Technology, Forestry Faculty, Duzce University, Duzce, Turkey; c: Department of Wood Mechanics and Technology, Forestry Faculty, Istanbul University, Bahcekoy, Sariyer, 34473, Istanbul, Turkey; \* Corresponding author: [addogu@istanbul.edu.tr](mailto:addogu@istanbul.edu.tr)

### INTRODUCTION

Wood modification can be defined as a process that improves the properties of wood, producing a new material that does not present any environmental hazard greater than unmodified wood when disposed at the end of its product life cycle (Hill 2006).

Thermal compression of wood is a modification method that combines thermal and mechanical processes, resulting in densification of wood. Depending on process conditions, a thermal compression process could also affect drying speed, equilibrium moisture content, hygroscopicity, dimensional stability, durability, surface quality, modulus of rupture, modulus of elasticity, Janka hardness, surface abrasion, strength, nail/screw withdrawal strength, and the shear modulus of wood (Tabarsa 1995; Navi and Girarde 2000; Kubojima et al. 2003; Blomberg et al. 2005; Wang and Cooper 2005a;

Unsal and Candan 2007; Yoshihara and Tsunematsu 2007; Welzbacher et al. 2008; Unsal et al. 2009).

Densified wood, which has high density, strength, and dimensional stability, can only be attained if all the relevant characteristics of wood (structural, chemical, physical, mechanical, rheological, etc.) are considered (Kutnar and Šernek 2007).

During the thermal compression process, solid wood is exposed to compressive stresses in radial or tangential directions, in addition to temperature effects. A number of studies have reported that wood behavior in transverse compression is dependent on its anatomical features (Bodig 1965; Kunesh 1968; Easterling et al. 1982; Alexiou 1994; Stefansson 1995; Ando and Onda 1999; Tabarsa and Chui 2000; Burgert et al. 2001; Tabarsa and Chui 2001; Müller et al. 2003; Gong et al. 2006; Nairn 2006). Studies also show that wood responds differently to radial and tangential compression because of its anisotropic nature (Kunesh 1961; Dinwoodie 1965; Kennedy 1968; Boding and Jayne 1982; Dinwoodie 2000; Tabarsa and Chui 2001; Walther 2003; Wang and Cooper 2005b).

Changes in the anatomical structure of wood at various temperatures have been studied in detail (Fengel and Wegener 1989; Terziev et al. 2002; Boonstra et al. 2006; Persson et al. 2006; Awoyemi and Jones 2010). Even though a considerable amount of research has focused on the chemical, mechanical, and physical properties of thermally compressed wood and changes in the anatomical structure of wood at different compressive stresses or temperatures, there is a lack of information on the changes in the microstructure of various wood species subjected to thermal compressing process. It is important to know how anatomical structure of wood is affected by modification methods, since changes are likely to affect the mechanical behavior and strength properties of wood products in end use applications.

The objective of this study was to evaluate the effects of varying temperatures and press pressures on the anatomical structure of solid-wood panels produced by using *Pinus sylvestris* L. (Scotch pine) wood.

## EXPERIMENTAL

### Materials

This study was performed by using wood samples obtained from different thermal compression processes. Commercial Scotch pine (*Pinus sylvestris* L.) solid panels having no defects with dimensions of 250 by 500 by 18 mm were hot-pressed using a laboratory hot press at a temperature of either 120°C or 150°C and pressure of either 5 or 7 MPa for 60 min (Table 1). A total of 10 panels, two for each treatment group, were used. The panels were pre-dried to a moisture content of 19% before hot-pressing. In this process, panel thickness decreased to 11 mm and average moisture content decreased to 8.6% by using the maximum pressure of 7 MPa. No defects and deformations occurred macroscopically at the end of the hot-press processes (Unsal and Candan 2008). On the other hand, darkening of boards was quite noticeable for the 150°C-7 MPa process condition.

**Table 1.** Process Parameters of Treatment Groups

Group	Pressure (MPa)	Temperature (°C)	Duration (min)
Control	—	—	—
A	5	120	60
B	7	120	60
C	5	150	60
D	7	150	60

## Methods

Light Microscopy (LM) and Scanning Electron Microscopy (SEM) were employed to reveal deformations in the anatomical structure of the panels subjected to varying thermal compression conditions. Small wood samples were obtained from the outer region of sapwood in order to eliminate possible effects of juvenile wood and heartwood, which are likely to be present in wood samples. Samples with dimensions of 10 mm (R) x 10 mm (T) x 20 mm (L) were cut for LM evaluations. These samples were kept under vacuum in the presence of alcohol, glycerin, and water at room temperature in order to become softened and were then cut into thin sections (about 30  $\mu\text{m}$ ) by using a Reichert sliding microtome. The microtome knife was often changed to minimize surface roughness and any possible damage on the surfaces of the samples. The sections were then stained with safranin and fast green to supply good contrast between cell walls and thus to get clear observations of changes in the wood structure. The sections were observed under an Olympus BX51 Light Microscope. Images were taken by using analySIS FIVE Software and a DP71 Digital Camera installed and adapted on the microscope.

Since microscopic investigations indicated some differences in micro-structural appearances in Group D samples during the course of thermal compression in this study, the samples were divided into two sub-groups, and their characteristics were described separately. The first sub-group D<sub>1</sub> showed visually wider growth rings and earlywood layers, with an almost gradual transition from earlywood to latewood. The second sub-group, D<sub>2</sub>, showed narrow and uniform growth rings with rather narrow latewood layers, and abrupt transition as well. SEM observations were, therefore, carried out for the Group D subjected to the most severe condition of the process in terms of temperature and pressure in order to better understand the properties of this group. SEM observations were also performed for the untreated wood samples for comparison purposes. The small wood samples with the dimensions of 10 mm (R) x 10 mm (T) x 10 mm (L) were cut for SEM analyses. SEM samples were cut with a razor blade to obtain smooth surfaces. The samples were then transferred directly to a Hitachi Tabletop Microscope TM-1000 without metal coating.

Anatomical investigations were also performed for untreated wood samples for comparison purposes. All microscopic studies were realized visually only on cross sections, radial sections, and tangential sections.

## RESULTS AND DISCUSSION

Microscopic investigations performed on the each treatment group were evaluated together for cross section, radial section, and tangential section to better understand the effects of temperature and press pressure on the anatomical structure of the wood. Images of untreated wood samples are shown in Fig. 1 (LM) and Fig. 2 (SEM) for comparison.

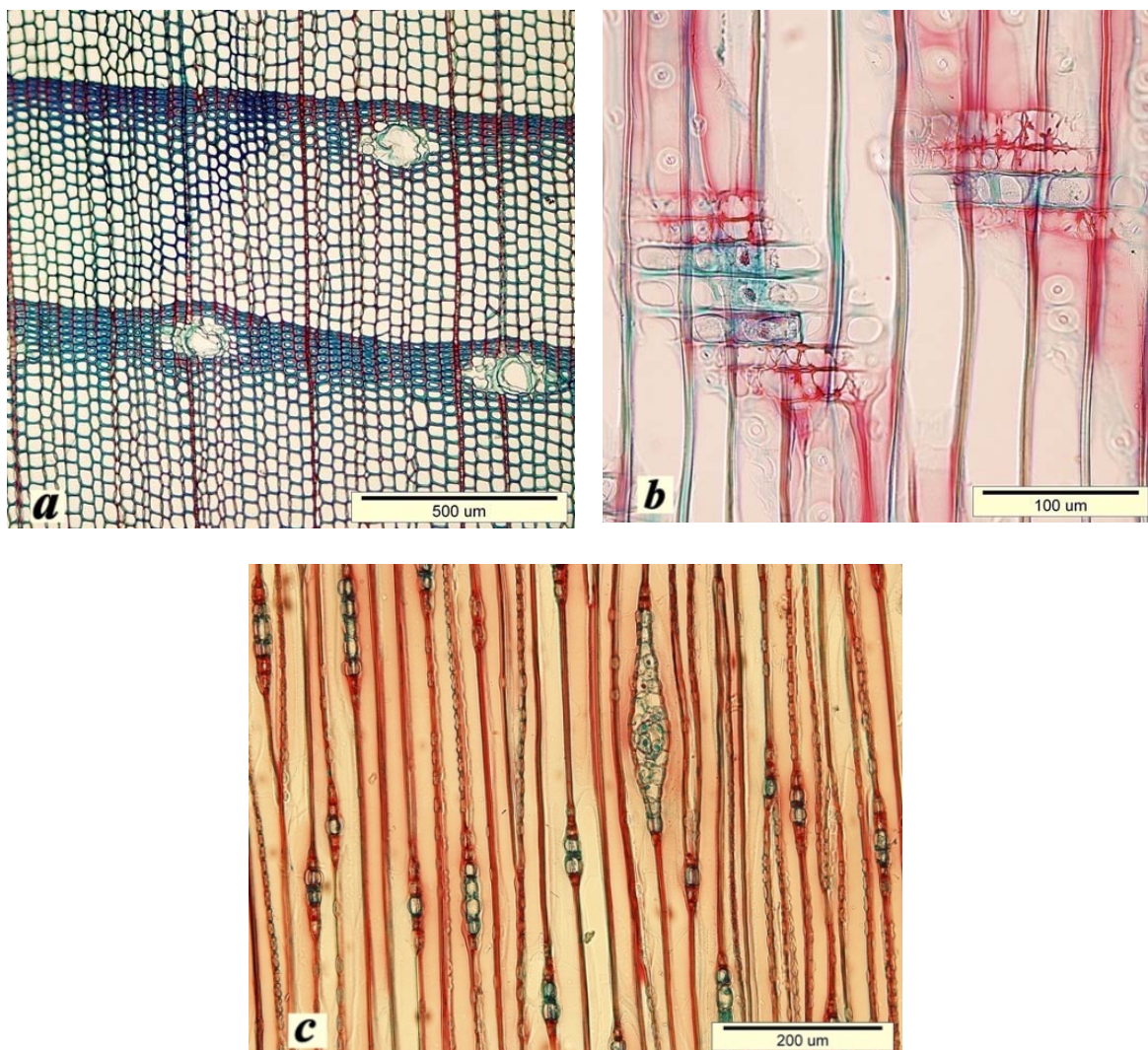


**Fig. 1.** Light micrographs of untreated wood: a) Cross section, b) Radial section, c) Tangential section

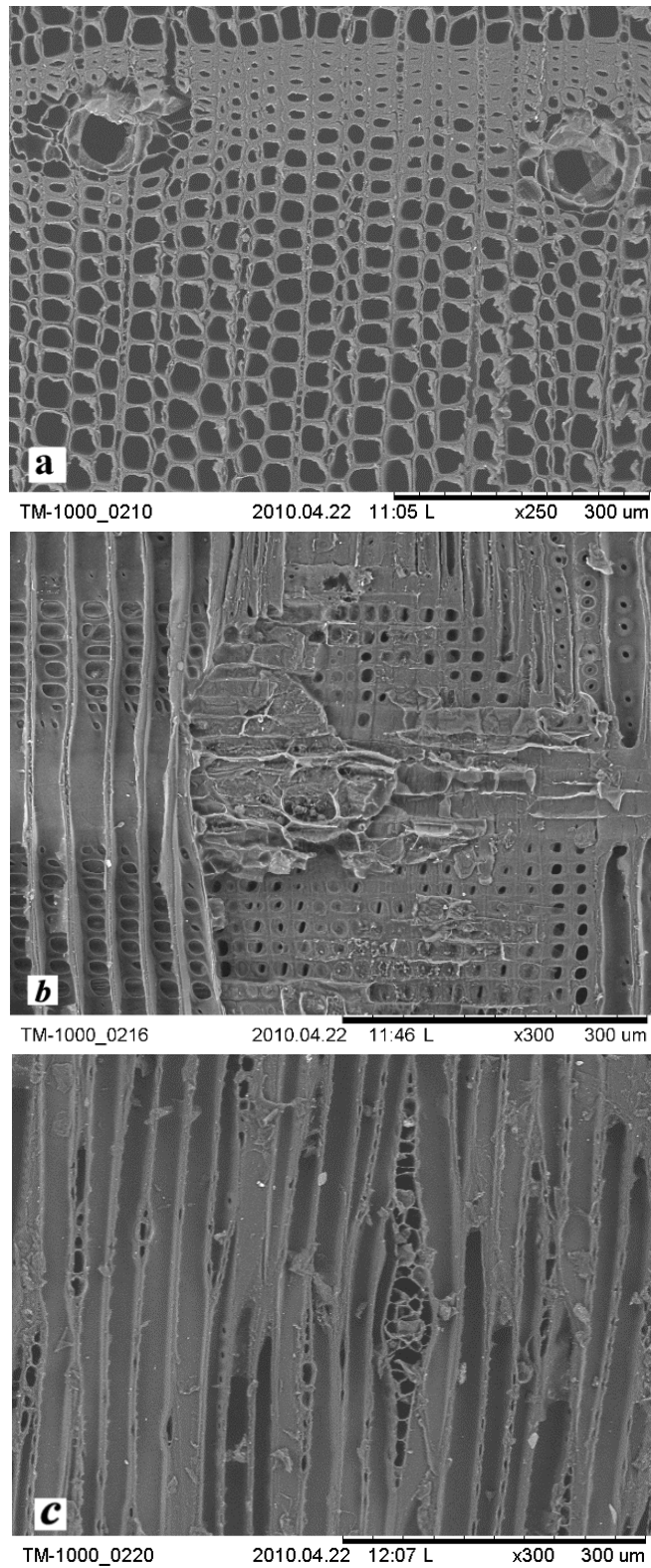


**Fig. 2.** SEM micrographs of untreated wood: a) Cross section, b) Radial section, c) Tangential section

### Cross Section

Depending on the effects of varying temperatures and press pressures, growth rings showed different structural distortions in the test groups. Since the Group A samples (120°C – 5 MPa) showed minimum structural damage, no visible distortion in the plane of growth rings was observed (Fig. 3a). A slight shift in the radial direction of the growth rings was observed in Group C (150°C – 5 MPa) (Fig. 3c). Even though Group B (120°C – 7 MPa) and sub-group D<sub>2</sub> (150°C – 7 MPa) exhibited only wavy structure in the earlywood regions, sub-group D<sub>1</sub> (150°C – 7 MPa) showed the similar structure throughout the all annual rings (Fig. 3b, Fig. 3d, Fig. 3e, Fig. 3f and Fig. 3g).



**Fig. 3.** a) No visible distortion in the plane of growth rings, radial cracks along the rays (arrows 1), axial resin canals in circular shape and damaged epithelial cells around these canals (arrows 2) in Group A, b) Buckling on the radial cell walls of the earlywood tracheids and wavy pattern in relevant regions (arrow 1), and axial canals in circular shape (arrow 2) in Group B, c) Slight shift in radial direction of the growth rings, rays in narrow nodular shape (arrow 1), axial resin canals almost in circular shape and damaged epithelial cells around these canals (arrow 2) in Group C

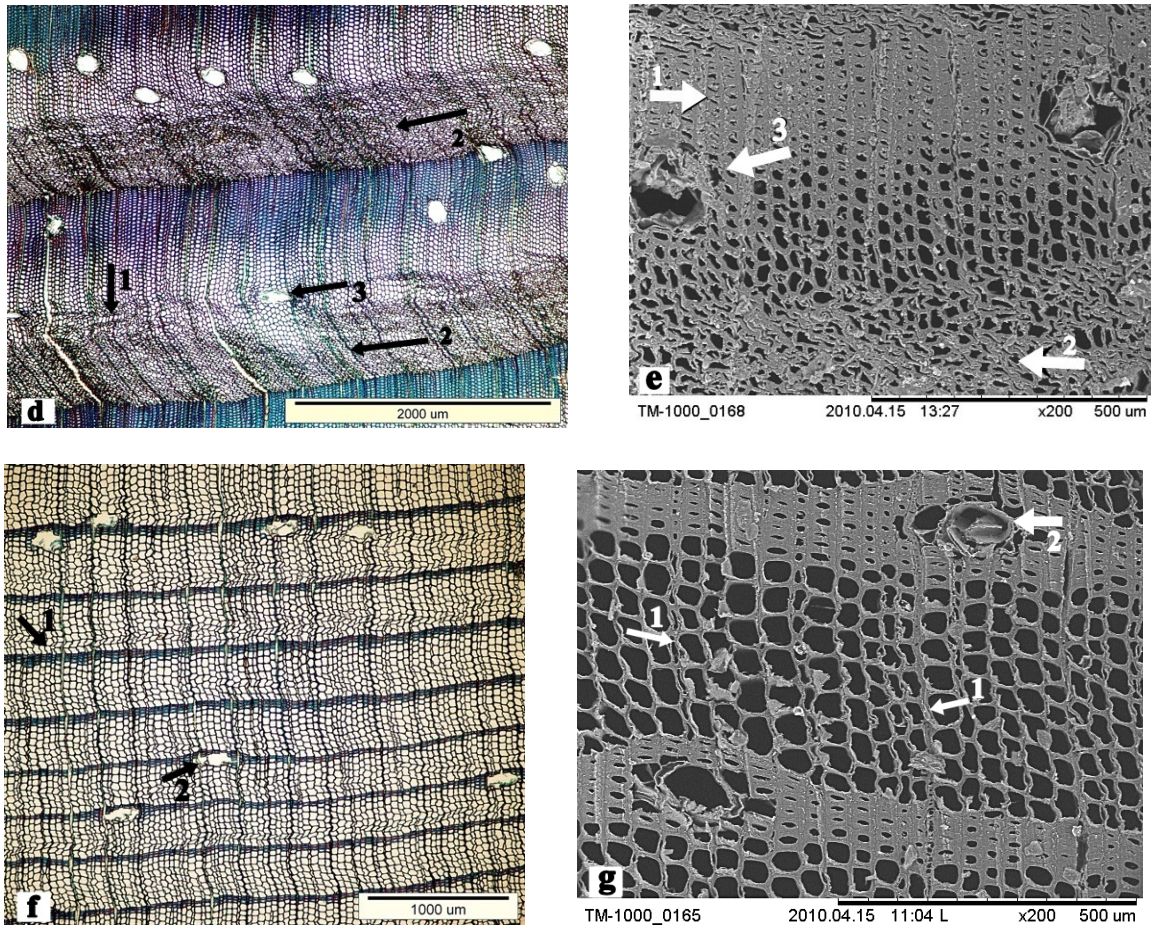


**Fig. 3** (continued). d) Cell collapse in earlywood tracheids and latewood tracheids without cell collapse (arrow 1), growth rings in wavy pattern and rays in zigzag shape (arrow 2), axial resin canals with flat shape in radial direction in the collapse area of sub-group D<sub>1</sub> (arrow 3), e) Compressed latewood region (arrow 1), collapsed earlywood region (arrow 2), and damaged axial resin canal in sub-group D<sub>1</sub> (arrow 3), f-g) Growth rings without collapse and wavy structure in most parts of earlywood regions, rays in wavy structure (arrow 1), axial resin canals compressed in radial direction in latewood regions of sub-group D<sub>2</sub> (arrow 2)

Minute cracks were observed in the cell wall of earlywood tracheids, and some degradation in the inner layer of the secondary walls of these cells were noticed particularly in the initial part of the growth rings for Groups A, B, and C (Figs. 4a-c). On the other hand, minute cracks and severe degradation were observed in the secondary walls of almost all tracheids in the earlywood for Group D (Figs. 4d and 4e).

Buckling on the radial cell walls of the earlywood tracheids were found clearly in a few cell rows behind the growth ring border in Group B. These structural alterations on the earlywood tracheids resulted in a wavy pattern in the relevant regions (Fig. 3b). Fractures were also observed in some cell walls near the earlywood tracheid corners in the initial part of the growth rings (Fig. 5a). This was considered as an initial stage of cell collapse. While ruptures were found in the secondary walls of the earlywood tracheids in the initial part of the growth rings for all groups, a great number and more distinct ruptures were observed in Group C and sub-group D<sub>2</sub> (Fig. 4c and Fig. 5b).

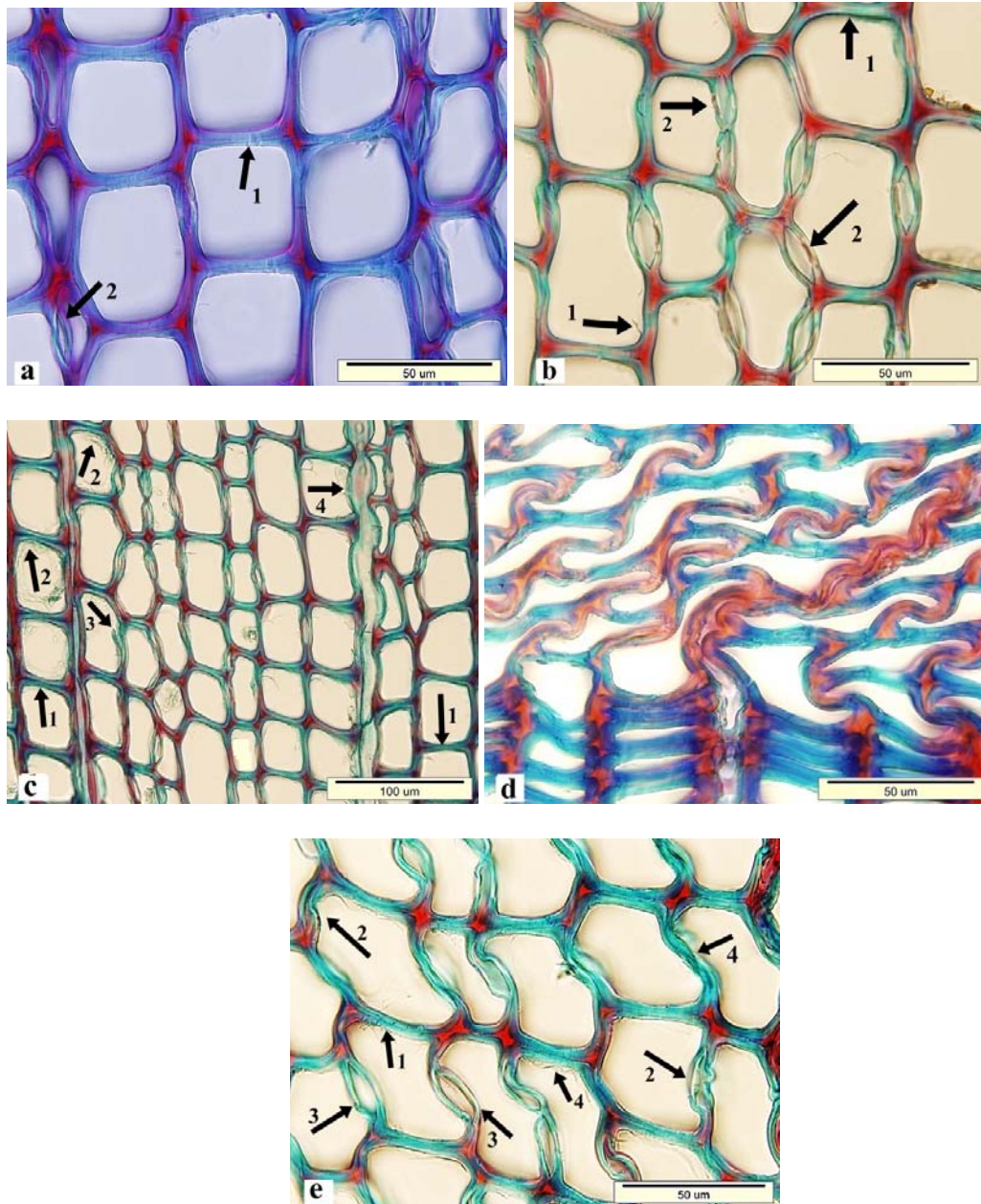


**Fig. 4.** a) Minute cracks in the cell wall of earlywood tracheids (arrow 1) and slight damage in bordered pits of Group A (arrow 2), b) Minute cracks in the cell walls of the earlywood tracheids and some degradation in the inner layers of the secondary walls (arrow 1), ruptured and/or aspirated bordered pits expanded in tangential direction in Group B (arrow 2), c) Minute cracks (arrow 1), cell walls degradation (arrow 2) and ruptures (arrow 3) in the secondary walls of the earlywood tracheids in the initial part of the growth ring and rays in narrow nodular shape (arrow 4) in Group C, d) Severe degradation in the cell wall of earlywood tracheids in the collapse area of sub-group D<sub>1</sub>, e) Buckling of the radial cell walls of earlywood tracheids, minute cracks in the cell walls (arrow 1), and separations between compound middle lamella (arrow 2), damaged bordered pits expanded in tangential direction in the earlywood region (arrow 3), severe degradation in the secondary walls of earlywood tracheids (arrow 4) in sub-group D<sub>2</sub>

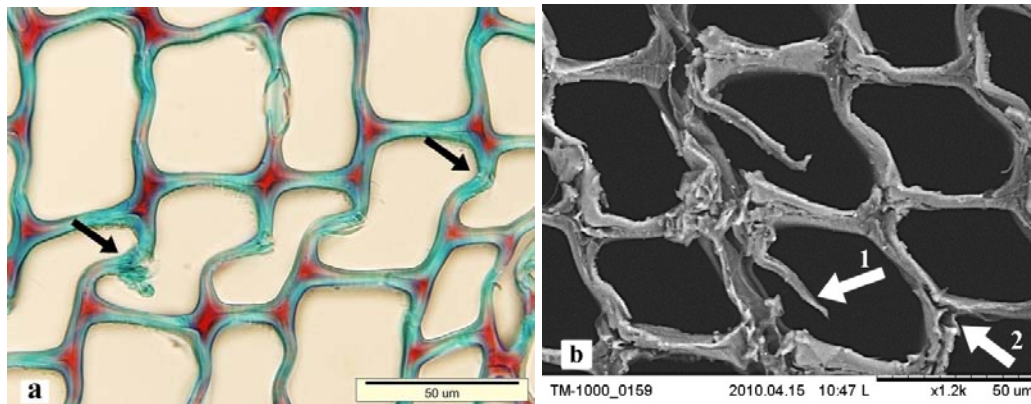


**Fig. 5.** a) Fractures in some cell walls near the earlywood tracheid corners in Group B, b) Ruptures in the cell walls (arrow 1) and separations between compound middle lamella in earlywood region of sub-group  $D_2$  (arrow 2)

Cell collapse occurred in almost all earlywood tracheids, whilst it was not observed in latewood in sub-group  $D_1$  (Fig. 3d and Fig. 6a). Although the earlywood tracheids collapsed into different shapes, their lumina were usually not closed due to strong resistance present in the cell corners (Fig. 3e, Fig. 4d and Fig. 6a). Since the compressed cell zones were followed by the uncompressed cell zones, growth rings appeared in a wavy pattern (Fig. 3d and Fig. 6a). Severe degradation was observed in the secondary walls of almost all tracheids in the earlywood in sub-group  $D_1$  (Fig. 4d). No cell collapse occurred in sub-group  $D_2$ ; however, large cell wall deformation was observed in all growth rings (Fig. 3g and Fig. 6b). Radial walls of the earlywood tracheids buckled toward the cell lumen (Fig. 3g and Fig. 4e). It was thought that the buckling of radial cell walls was an indication that abrupt fractures would occur. Because of the buckled radial cell walls, wavy structure was observed in most parts of the earlywood regions. Separations between compound middle lamella were observed in the earlywood tracheids. Minute cracks were also seen in the cell walls (Fig. 4e and Fig. 5b).

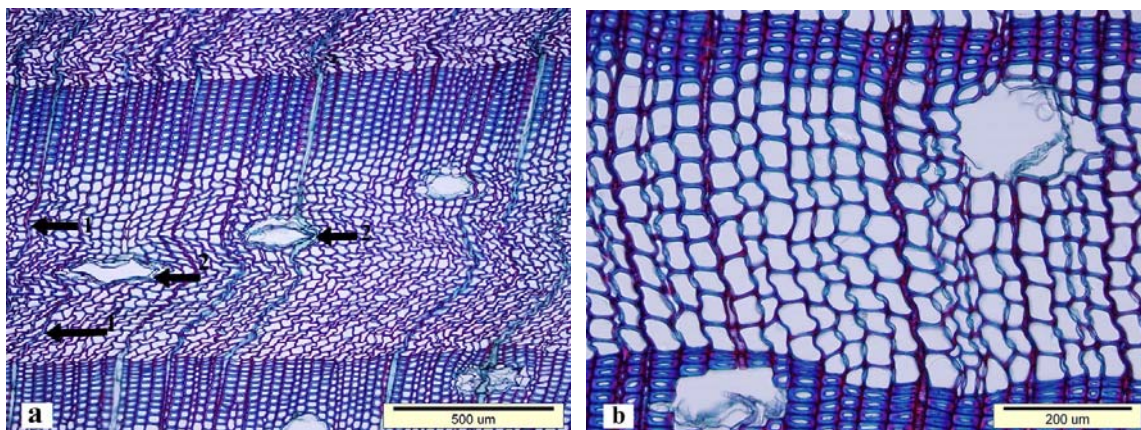


**Fig.6.** a) Cell collapse in earlywood tracheids and latewood tracheids without cell collapse, growth rings in wavy pattern and rays in zigzag shape (arrow 1), axial resin canals with flat shape in radial direction in the collapse area of sub-group  $D_1$  (arrow 2), b) Large cell wall deformation without cell collapse in the all growth ring of sub-group  $D_2$

Depending on the process conditions, more or less distinct cracks were seen in the cell walls of the latewood tracheids for all groups except Group D (Fig. 7a, Fig. 7b, Fig. 7c, Fig. 7d, Fig. 7e and Fig. 7f). Cracks were in large quantities and quite distinct in Group B. Splits were also observed in some cell walls near the latewood tracheid corners in Group C (Fig. 7c). Some separations were observed between those cells in the tangential direction for the same groups as they were in case of crack formation (Fig. 7a, Fig. 7b and Fig. 7c).

On the other hand, the distance between the cells seemed to be decreased in Group B and Group C, and separations disappeared in Group D (Fig. 7d, Fig. 7e and Fig. 7f). It was assumed that this probably occurred because of the latewood tracheids' pushing each other in the radial direction, depending on increasing compressive effect. Since such separations between latewood tracheids were also noticed in the untreated wood as well, this phenomenon was not attributed to the thermal compressing procedure. It was concluded that these types of separations might have been caused either by cutting with the sharp microtome-knife or by conditioning of solid wood panels.

Cell wall degradation in the latewood tracheids was observed mainly around axial resin canals in Group A-C (Fig. 8). Slight degradation was observed in the inner layers of the secondary walls of latewood tracheids in sub-group D<sub>1</sub> (Fig. 7d), whilst severe degradation was seen in almost all secondary cell walls in the latewood regions of sub-group D<sub>2</sub> (Fig. 7e). The linear structure of the latewood tracheid rows curved slightly, in particular near the axial resin canals with damaged epithelial cells in Group B and Group C (Fig. 8).

Distinct radial cracks along the rays were only noticed in Group A, but these types of cracks were also found in untreated wood (Fig. 3a). Therefore, this phenomenon was not attributed to thermal compressing procedure. No radial cracks along the rays were seen in Group B and C; however, some slight separations were observed in these groups. Moreover, rays in narrow nodular shape were observed in some regions of the earlywood (Fig. 3c and Fig. 4c). Ray parenchyma cells showed no cell collapse in sub-group D<sub>1</sub>, but compression of wood in the radial direction deformed the rays in zigzag shape in the earlywood (Fig. 3d and Fig. 6a). Rays in sub-group D<sub>2</sub> were wavy in earlywood regions and this appearance might be considered as the effect of pressure of buckled adjacent tracheids over ray parenchyma (Fig. 3f).

Axial resin canals in Group A-C were almost in their normal circular shape, whilst thin-walled epithelial cells around these canals seemed to be damaged (Fig. 3a, Fig. 3b, Fig. 3c, Fig. 3d and Fig. 3f). Since cell collapse occurred in almost all earlywood regions in sub-group D<sub>1</sub>, axial resin canals were flattened in radial direction (Fig. 6a). On the other hand, axial resin canals in the latewood were compressed in radial direction in sub-group D<sub>2</sub>. This was likely a result of the latewood tracheids' pushing each other in the radial direction (Fig. 3f and Fig. 3g).

Both undamaged and damaged bordered pits were found in the tracheid walls for Group A (Fig. 4a). However, bordered pits were expanded in tangential direction as pressure increased in Group B-D. A great number of ruptured and/or aspirated bordered pits were observed in the earlywood in these groups (Fig. 4b, Fig. 4c and Fig. 4e).

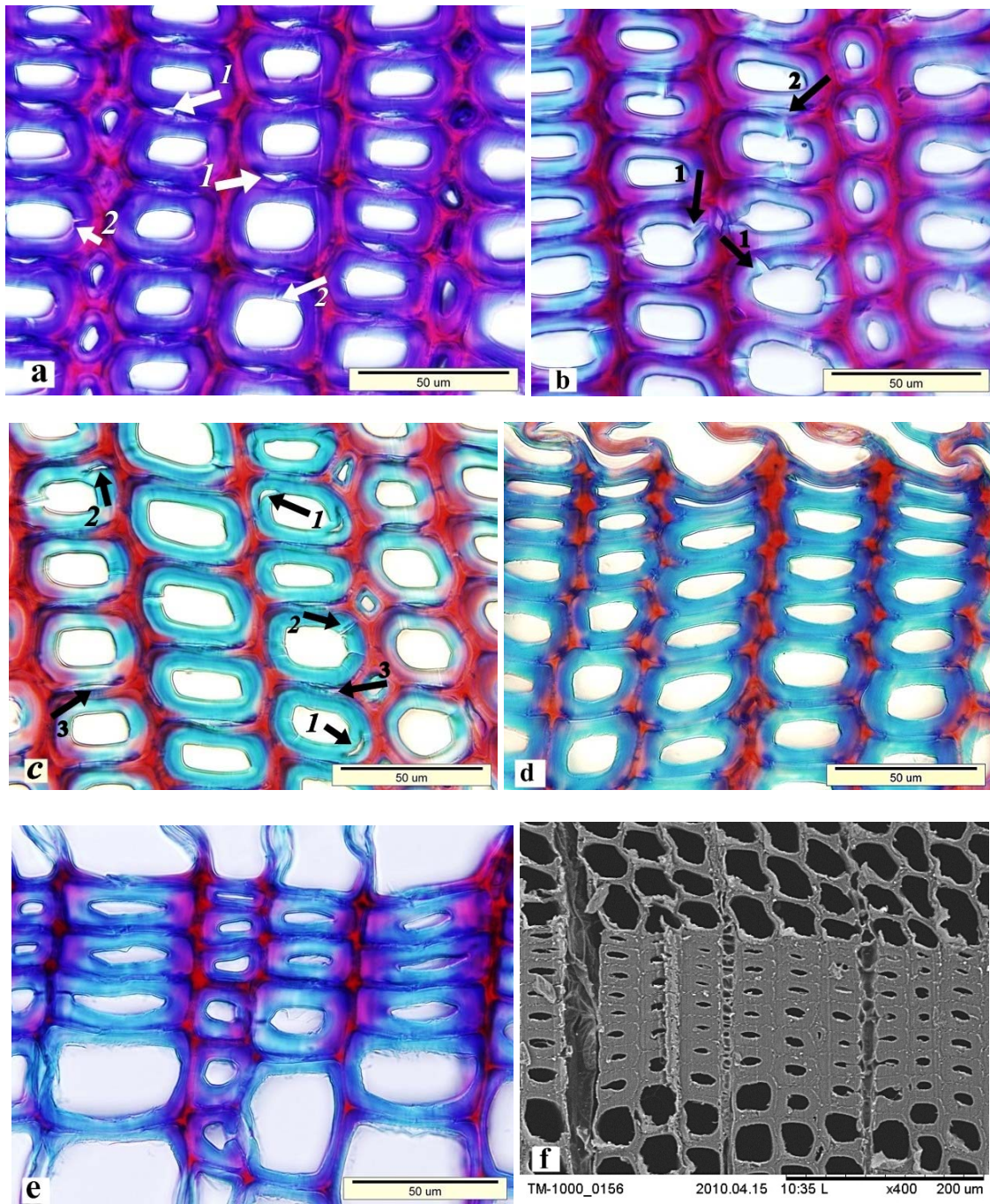


**Fig. 7.** a) Cracks in the latewood tracheid cell walls (arrow 2) and separations between these cells in Group A (arrow 1), b) Cracks in large quantities and quite distinct in the latewood tracheid walls (arrow 1) and separations between these cells in Group B (arrow 2), c ) Splits in some cell walls near the latewood tracheid corners (arrow 1), more or less distinct cracks in some cell walls (arrow 2) and separations between these cells in Group C (arrow 3), d) No cracks but little degradation in the inner layers of the secondary walls of latewood tracheids in sub-group D<sub>1</sub>, e) Severe degradation in the secondary walls of latewood tracheids without cracks, no visible separation between latewood tracheids in sub-group D<sub>2</sub>, f) No crack in latewood tracheid walls, and no separation between these cells in sub-group D<sub>2</sub>

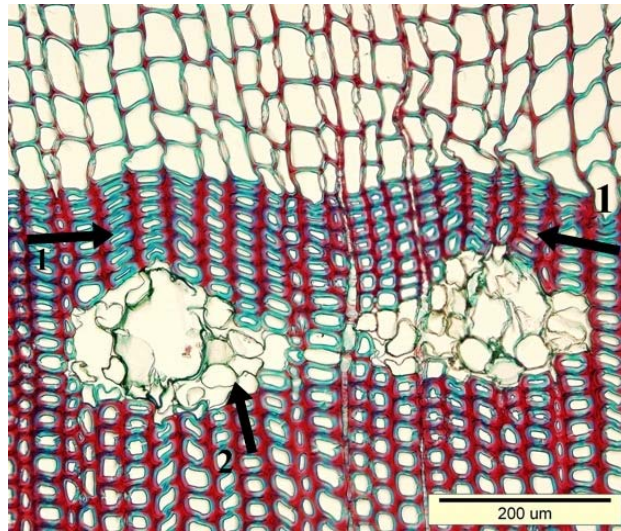


**Fig. 8.** Slight curvature in the latewood tracheid rows near the axial resin canals (arrow 1), cell wall degradation in the latewood tracheids around these canals in Group B (arrow 2)

### Radial Section

No visible changes were in the cell orientations of earlywood regions in Group A and C; however, changes were more distinctive in group B as pressure increased. Furthermore, latewood tracheids were little more compressed in Group B due to the effect of increased pressure when compared to the Group A and C. On the other hand, the high extent of compression effect was observed only in the latewood regions of sub-group D<sub>2</sub> (Fig. 9c), this effect was seen particularly in the collapsed earlywood regions of sub-group D<sub>1</sub> (Fig. 9a). Also, cell walls in the wood tissue showed a loose structure in sub-group D<sub>1</sub>. Thus, all cell walls showed an expanded form (Fig. 9b).

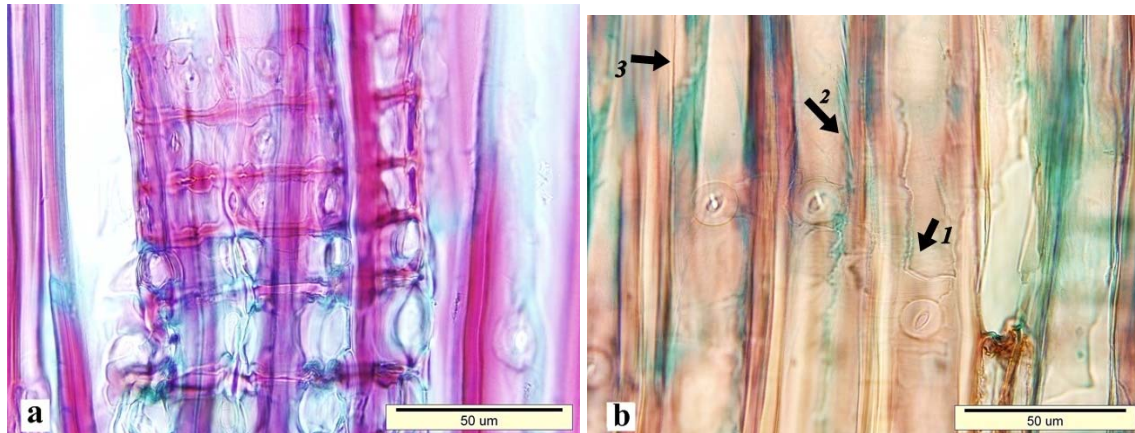


**Fig. 9.** a) Horizontally compressed ray parenchyma cells and ray tracheids in sub-group D<sub>1</sub>, b) Transwall crack (arrow 1), intrawall crack (arrow 2) and intercell crack (arrow 3) in radial walls of earlywood tracheids, loose structure in the cell walls of sub-group D<sub>1</sub>

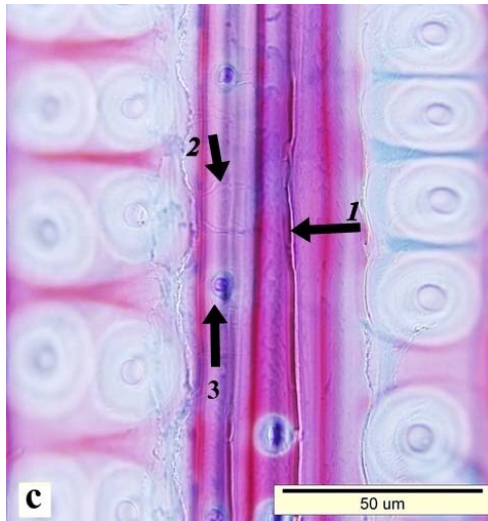


**Fig. 9** (continued). c) High extent compression effect in latewood region and intercell crack (arrow 1), minute transwall crack (arrow 2) and degradation in the radial cell walls of latewood tracheids, bordered pits without split-like appearance in latewood regions of sub-group D<sub>2</sub> (arrow 3)

Partial or complete destruction of tracheid lumen walls was detected in the radial cell walls of some earlywood tracheids in all groups. This type of destruction was observed less in untreated samples, and it was attributed to the effect of sharp microtome knife. However, the amount of destruction was greater than that in all groups. This was interpreted as the effect of process conditions. The cell walls of some earlywood tracheids showed more or less wavy pattern in all groups. It was also seen in the untreated samples. Therefore, it was not attributed to thermal compression (Fig. 10a). While the cell walls of some earlywood tracheids showed more or less degradation in Group A (Fig. 10b), the cell walls were almost degraded in some parts of the earlywood regions in Group B and C (Fig. 10c and Fig. 10d).

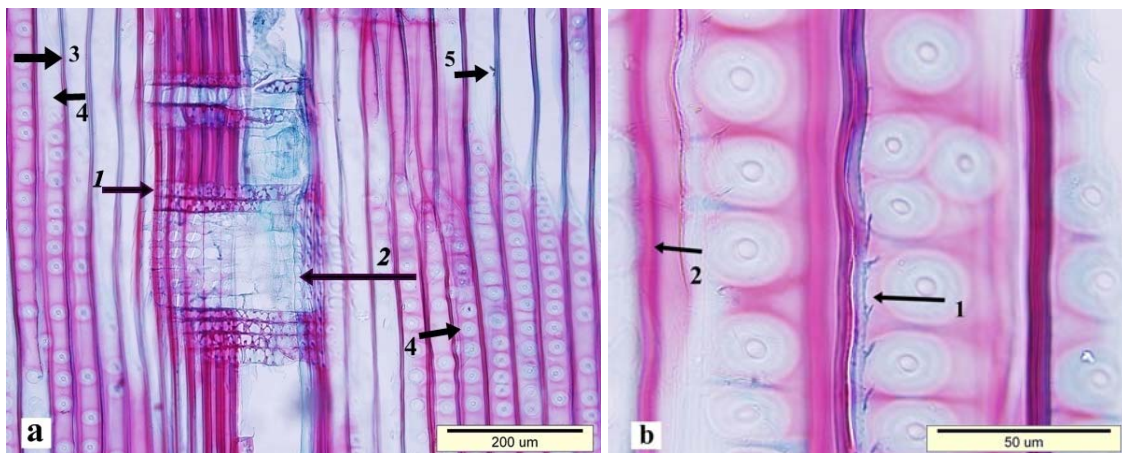


**Fig. 10.** a) Ray tracheids without damage (arrow 1), damaged ray parenchyma cells and damaged cross-field pits in earlywood region (arrow 2), slight wavy pattern in tracheids (arrow 3), damaged and undamaged bordered pits on the radial surfaces of tracheids (arrow 4), partial destruction of tracheid lumen walls in Group A (arrow 5), b) More (arrow 1) and less (arrow 2) degradation in the radial cell walls of the earlywood tracheids in Group A

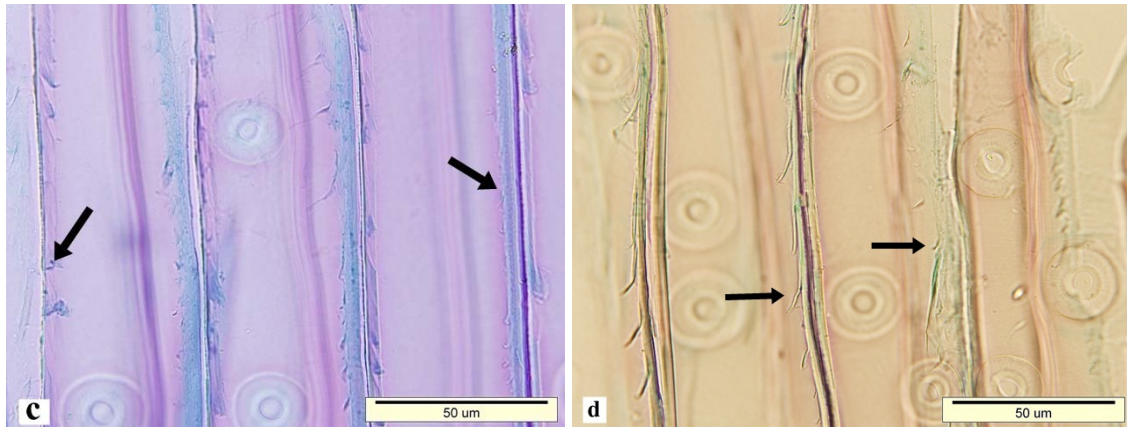


**Fig. 10** (continued). c) Degraded secondary cell walls of earlywood tracheids in Group B, d) Degraded secondary cell walls of earlywood tracheids in Group C.

Although intercell cracks and intrawall cracks were observed in the radial walls of the earlywood tracheids in Group A, minute transwall cracks were also detected in the other groups (Fig. 11a, Fig. 11b, Fig. 11c and Fig. 9b).

Cell wall degradation in the latewood tracheids were seen less in Group A and B than the other groups. Although Group A exhibited intercell cracks and intrawall cracks in the latewood tracheid cell walls, Group B and C showed also minute transwall cracks in those cell walls (Fig. 12a and Fig. 12b). No distinct crack was clearly seen in the cell walls of latewood tracheid in sub-group D<sub>1</sub>; however, minute transwall cracks and intercell cracks were detected in sub-group D<sub>2</sub> (Fig 9c).

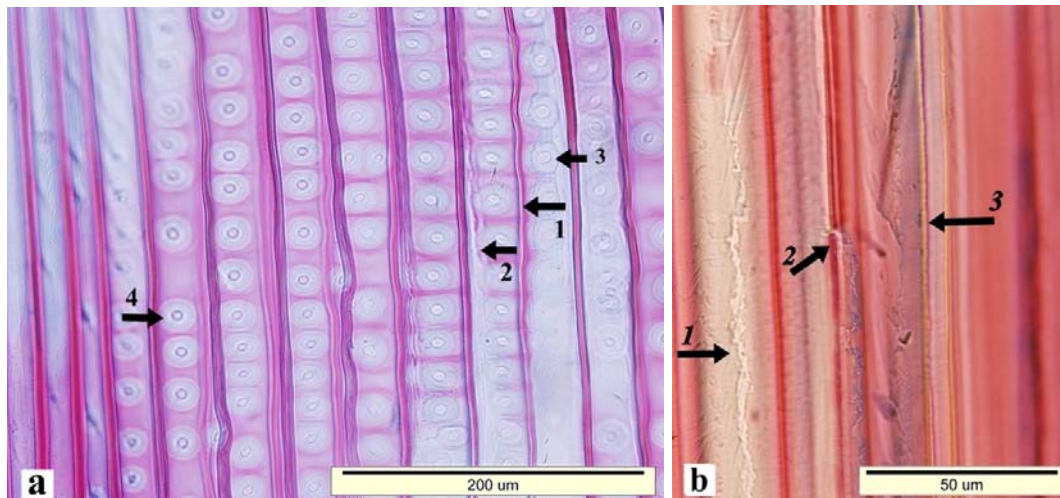


**Fig. 11.** a) Intercell crack (arrow 1) and intrawall crack (arrow 2) in radial walls of earlywood tracheids, damaged (arrow 3) and undamaged bordered pits (arrow 4) on the radial surfaces of tracheids in Group A, b) Intrawall crack (arrow 1), transwall crack (arrow 2) and intercell crack (arrow 3) in the radial walls of earlywood tracheids in Group B

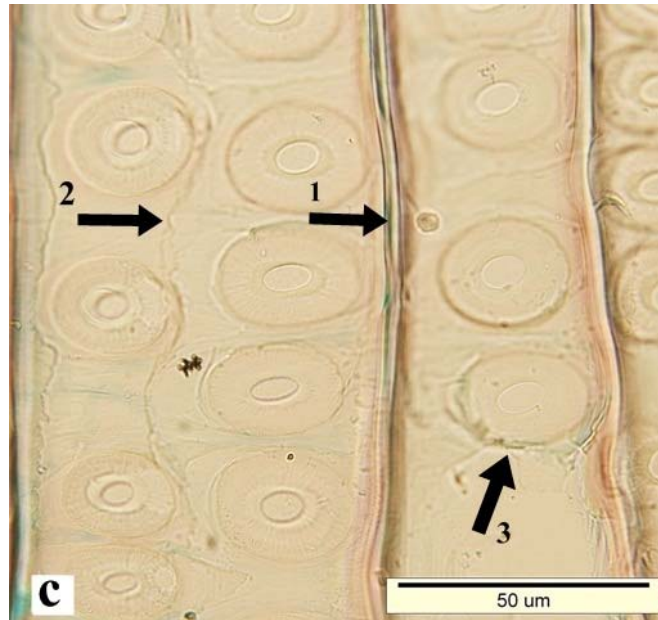


**Fig. 11** (continued). c) Intercell crack (arrow 1) and intrawall crack in tracheid walls (arrow 2) and damaged bordered pits (arrow 3) in Group C

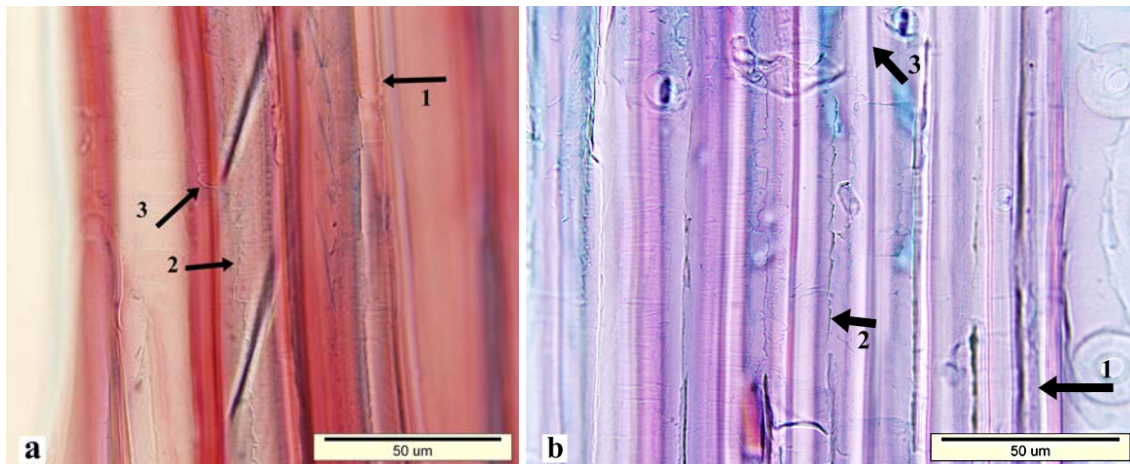


**Fig. 12.** a) Intercell crack (arrow 1), intrawall crack (arrow 2) and transwall crack (arrow 3) in radial walls of latewood tracheids in Group B, b) intercell crack (arrow 1), intrawall crack (arrow 2) and minute transwall crack (arrow 3) in radial walls of latewood tracheids in Group C

Intercell cracks were detected in the horizontal walls of ray parenchyma cells in all groups (Figs. 13a and 13b). Partial or complete destruction of ray tissues was detected in some fields of earlywood in the all groups (Figs. 13b and 13c). This type of destruction was observed less in untreated samples, and it was attributed to the effect of sharp microtome knife, as was the case in the destruction of the earlywood tracheid lumen walls. However, the amount of destruction was greater than that in all groups. This was interpreted as the effect of thermal compressing processes. In addition to destruction of ray tissues, ray parenchyma cell walls were partially damaged in some parts of the

earlywood regions in the Group A-C. On the other hand, ray parenchyma cells seemed generally damaged in both earlywood and latewood in Group D. However, ray tracheids were seen in better condition than ray parenchyma cells in all groups. Ray tracheids were only damaged where the lumen sides of the earlywood tracheid walls were destroyed (Fig. 10a and Fig. 13b). Ray parenchyma cells and ray tracheids in sub-group D<sub>1</sub> were considerably compressed horizontally in the collapsed area of the earlywood regions and less in the latewood regions (Fig. 9a).

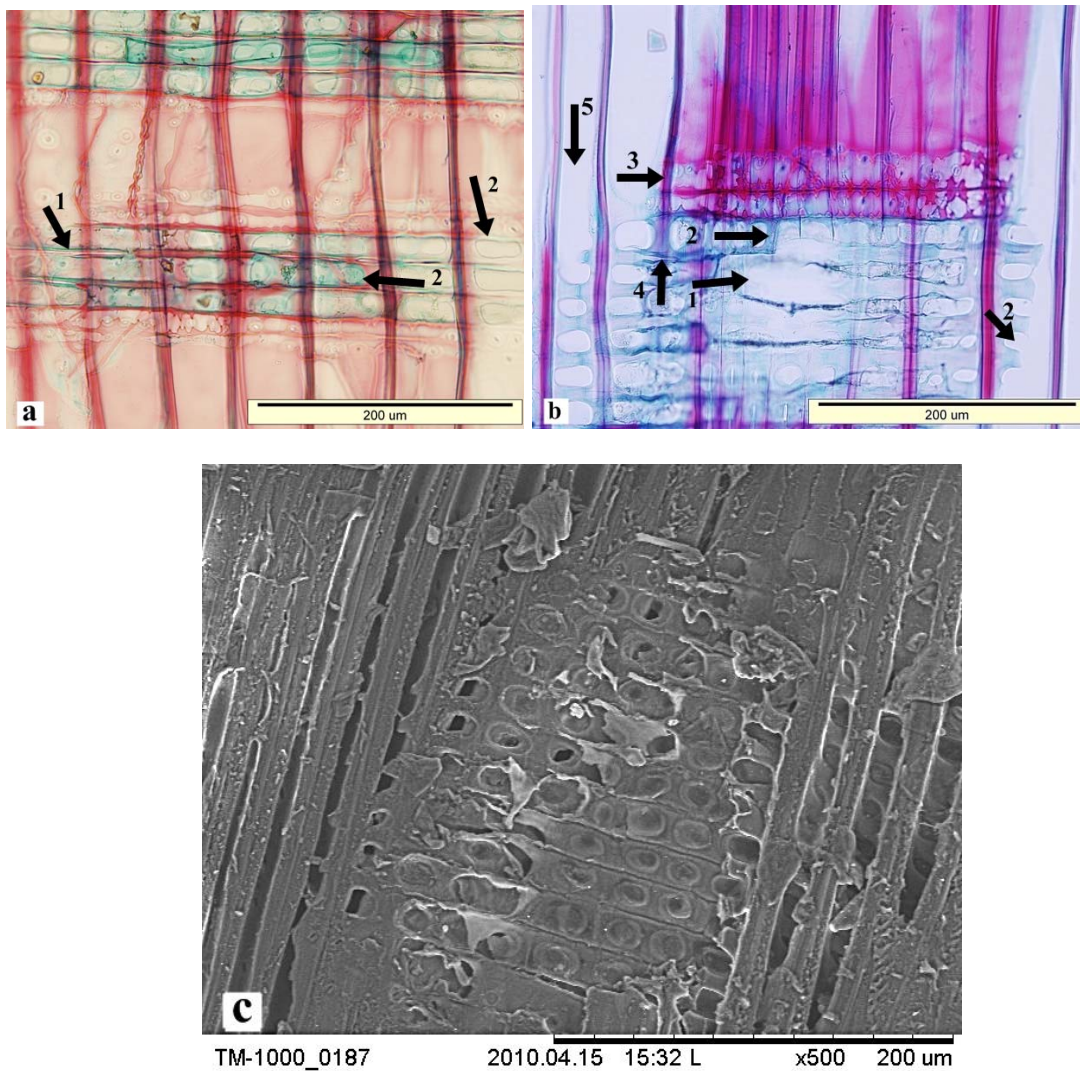


**Fig. 13.** a) Intercell cracks in ray parenchyma cells (arrow 1), cross-field pits in open structure with partly loosened or ruptured pit membranes in Group B (arrow 2), b) Damaged ray parenchyma cells (arrow 1) and cross-field pits (arrow 2) in the earlywood and latewood regions, ray tracheids in better condition than ray parenchyma cells (arrow 3), intercell crack in the horizontal walls of ray parenchyma cells (arrow 4) and destruction in ray tissues (arrow 5) of sub-group D<sub>2</sub>, c) Compressed ray parenchyma cells and ray tracheids in earlywood region, destruction in ray tissue and damage in tracheid walls of sub-group D<sub>1</sub>

It was thought that ray cells did not collapse by themselves but were compressed by pressure of adjacent cells. However, ray cells were only compressed horizontally in the latewood regions in sub-group D<sub>2</sub>, and the high extent of compression effect was observed only in these regions (Fig. 9c). Numerous cross-field pits in the earlywood showed an open structure with partly loosened or ruptured pit membranes in Group A-C (Fig. 10a and Fig. 13a), whilst cross-field pits exhibited generally severe damage in the compressed zones of Group D (Fig. 13b and Fig. 13c).

Both undamaged and damaged bordered pits and pit aspirations were found on the radial surfaces of the earlywood tracheids in the all groups (Figs. 10a, 11a, and 11c). Depending on process conditions, changes were seen visually both in number and damage degree in bordered pits. Changes in the number of aspirated pits were observed, as it was in case of damage formation in pits. Therefore, a great number of ruptured and aspirated bordered pits were observed in the earlywood regions of Group D. Pit apertures of bordered pits usually appeared split-like in latewood because of compression of tracheids in the radial direction in Group A-C (Figs. 14a and 14b); however, distinct split-like appearance was not observed in Group D (Fig. 9c).

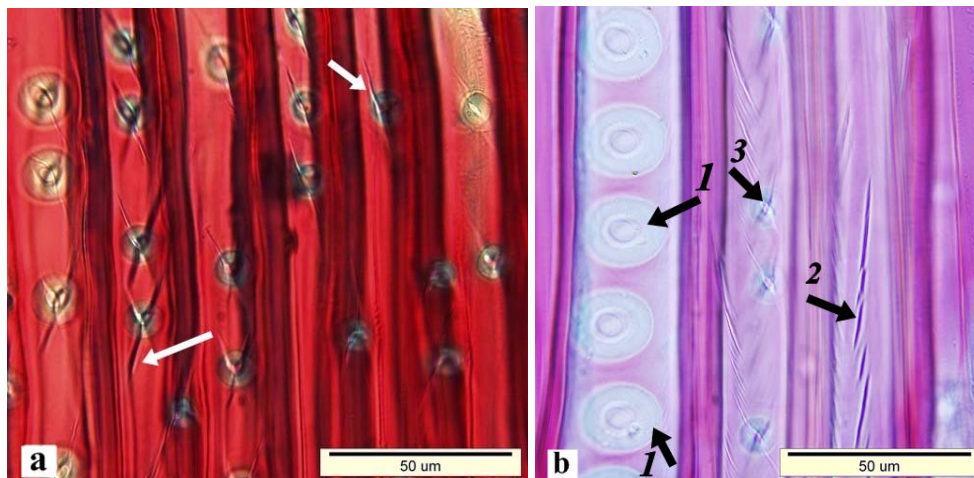


**Fig. 14.** a) Split-like pit apertures in latewood in Group A, b) Beginning of liquefaction of torus material with flowing along the margo fibrils (arrow 1), intrawall cracks in the radial walls of latewood tracheids (arrow 2), split-like pit apertures in latewood of Group B (arrow 3).

While there was a slight indication of the beginning of liquefaction of tori material, with flow occurring along the margo fibrils into the margo regions in Group B, there was more liquefaction in tori material in Group C (Fig. 14b and Fig. 15).

### Tangential Section

It was observed that the radial surface turned distinctly to the tangential surface where the earlywood tracheids seemed to be buckled in Group B (Fig. 16a); however, they turned rather slightly to the tangential surface in Group C. This might be a result of process pressure lower than Group B. The radial surfaces turned distinctly to tangential surfaces in earlywood due to severe process conditions in sub-group D<sub>1</sub> (Fig. 16b), whilst the turning of radial surface toward the tangential surface was not sharp in sub-group D<sub>2</sub>. On the other hand, Group A did not show such formation.

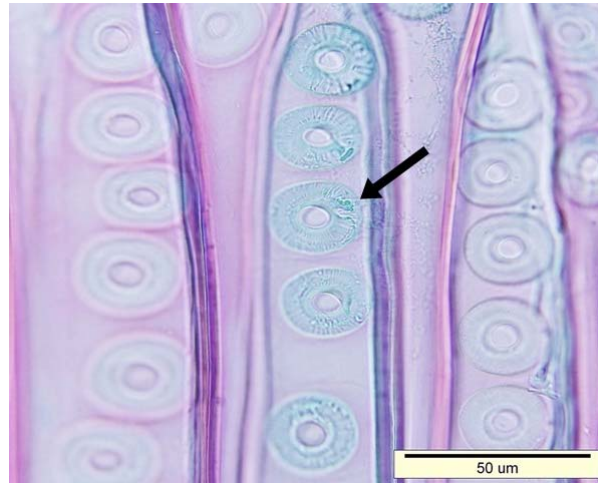


**Fig.15.** More liquefaction in tori material with flowing along the margo fibrils in Group C

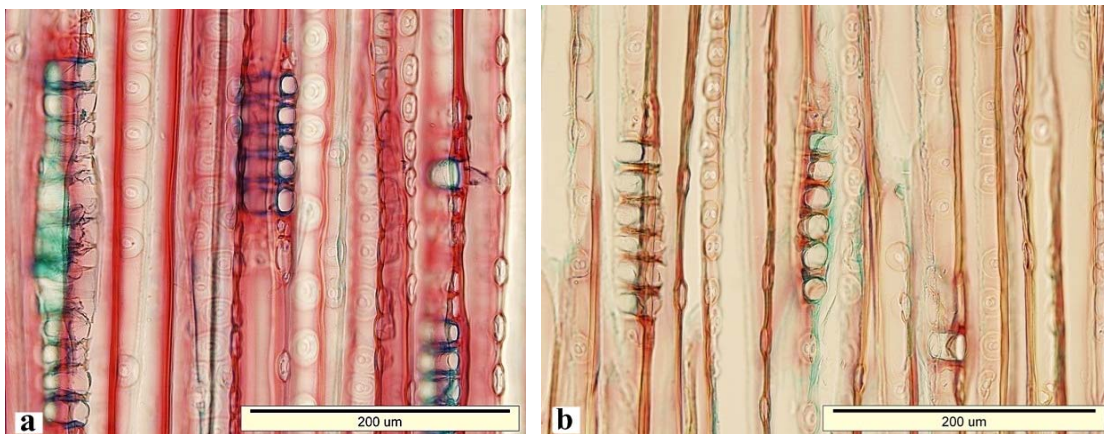


**Fig. 16.** a) The distinct turning of the radial surface to tangential surface in Group B, b) The distinct turning of the radial surface to tangential surface in sub-group D<sub>1</sub>

The microstructure of wood showed almost the same visual properties in the tangential sections as it was in case of radial sections (Figs. 17a, 17b, and 17c). Bordered pit membranes were encrusted by resin compounds in the earlywood regions of Group D (Fig. 17d). Axial resin canals appeared to be filled by the substances of epithelial cell walls in Group D (Fig. 17e).

This study showed that the highest deformation occurred in the earlywood regions of all growth rings for each process condition. Latewood regions exhibited less deformation than earlywood regions. This difference demonstrated that the distribution of deformation was not uniform in growth rings. It was evaluated that cell-wall thickness was an important factor in wood behavior during thermal compressing process.

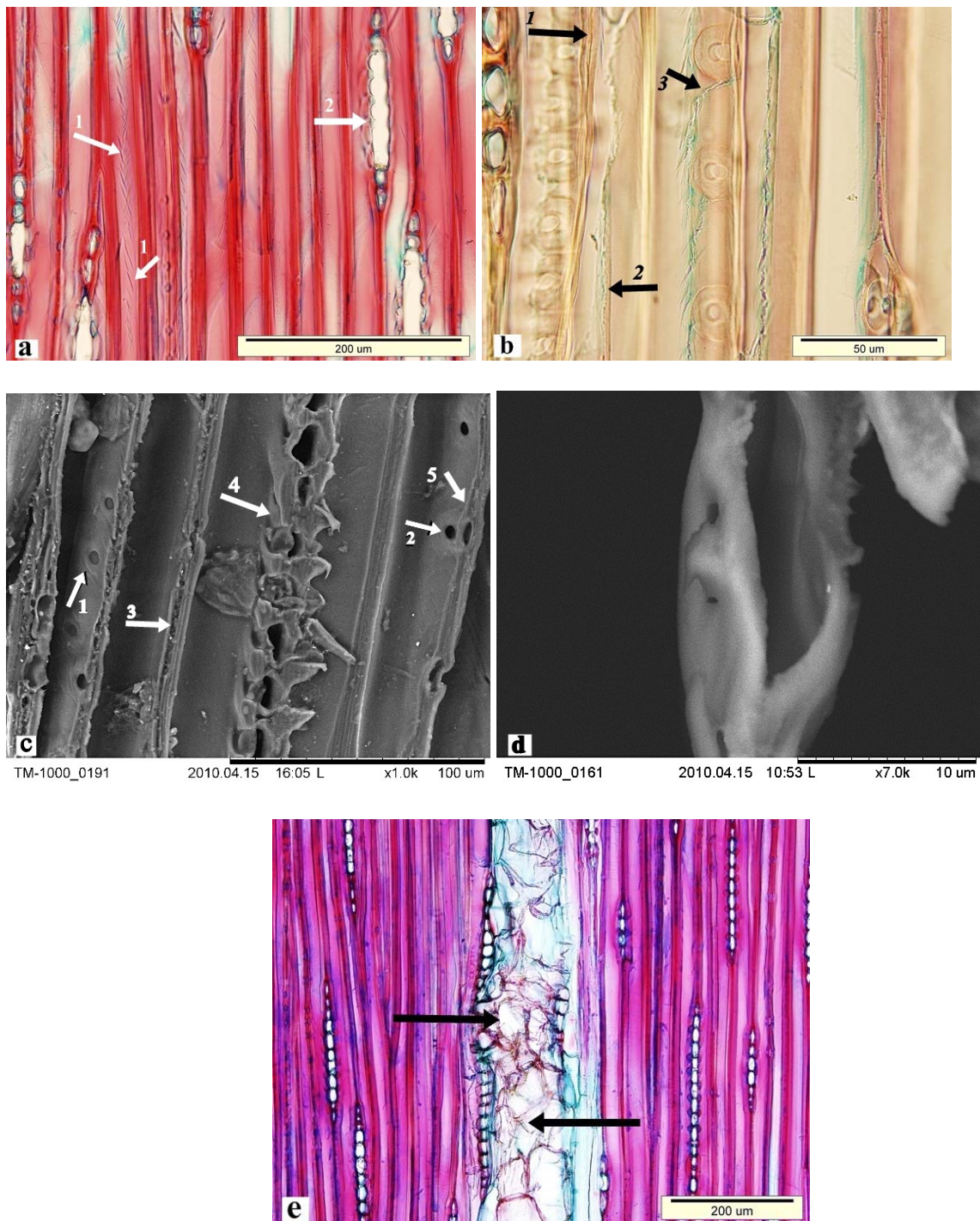


**Fig. 17.** a) Slight degradation and intrawall cracks in the tangential cell walls of the latewood tracheids (arrow 1), damaged and undamaged rays in Group A (arrow 2), b) Intercell crack (arrow 1), intrawall crack (arrow 2) and transwall crack (arrow 3) in the tangential cell walls of the earlywood tracheids, severe degradation in the tracheid cell wall of sub-group D<sub>1</sub>, c) Aspirated (arrow 1) and unspirated bordered pits (arrow 2), intercell crack (arrow 3), and intrawall crack (arrow 5) in the tracheid cell walls, damaged ray (arrow 4) in sub-group D<sub>1</sub>, d) Pit membranes encrusted by resin compounds in earlywood regions of Group D, e) Axial resin canals filled by the substances of epithelial cell walls in sub-group D<sub>1</sub>.

Bodig (1965) reported that the earlywood was responsible for compression behavior in softwoods under radial compression, and the first failure was found in this region. The results of both studies were consistent. The same findings were also obtained in other studies (Kennedy 1968; Kunesh 1968; Easterling et al. 1982; Stefansson 1995; Ando and Onda 1999; Tabarsa and Chui 1999; Burgert et al. 2001; Irle and Kwon 2001; Tabarsa and Chui 2001; Müller et al. 2003; Walther 2003; Gong et al. 2006).

During the thermal compressing process, buckling was found in the radial cell walls of a limited number of earlywood tracheids in Group B (120°C – 7 MPa) and occurred until the transition zone in Group D was reached (150°C – 7 MPa). The samples subjected to 5 MPa press pressure exhibited less deformation in wood structure at 120°C. It is clear that the impact of pressure in wood structure is promoted by increased temperature. The same pressure level had much more effect in the wood deformation at higher temperatures. This result was supported by the average density values, by the Janka hardness values of the solid wood panels, as found by Unsal and Candan (2008) in a previous study, and by the observed increase in density. The values showed an increase at the same pressure at higher temperature (Table 2).

In the present study, radial walls of the earlywood tracheids were detected as low strength regions where bordered pits were found, since buckling and ruptures were observed particularly in below and/or above of these regions.

Ray tracheids were more resistant to the process conditions than were ray parenchyma cells. It was considered that ray parenchyma cells were non-lignified in sapwood despite the fact the ray tracheids were lignified. Thus, the ray parenchyma cells were much more damaged at all temperature and pressure levels.

The results showed that the sub-groups D<sub>1</sub> and D<sub>2</sub> behaved quite differently from each other. This might be explained by different growth ring structure and different amount of latewood and earlywood in the samples. While sub-group D<sub>1</sub> showed cell collapse in the earlywood layers, sub-group D<sub>2</sub> showed no cell collapse. Some studies reported that the first collapse occurred in the weakest regions of the earlywood layers under radial compression (Bodig 1965; Kunesh 1968; Easterling et al. 1982; Stefansson 1995). Bodig (1965) and Kennedy (1968) found that the earlywood/latewood ratio was an important parameter for explaining the differences in behavior of wood under transverse compression. Kennedy (1968) and Tabarsa and Chui (2001) also noticed that species with low latewood percentage were stronger under radial compression. Sub-group D<sub>2</sub> in this study did not show any cell collapse in these regions when compared to the sub-group D<sub>1</sub> for the same process condition. It can be considered that the homogenous structure of growth rings with almost all of them uniform in earlywood and latewood widths throughout the wood samples plays a major role in prevention of cell collapse.

Wolcott et al. (1994) stated that when a majority of cells have collapsed, densification begins. In this context, significant densification began at the maximum temperature and pressure conditions in the current study, because almost all earlywood layers showed cell collapse. Kutnar and Šernek (2007) indicated that the increase in density is in the range of about 25% to about 500%, though preferably in the range of about 100% to about 200% in the densified wood. Results of the current study indicated that the percentage of maximum increase in density was 80%, in Group D (Table 2). However, the maximum density did not reach to preferred initial value of 100%.

**Table 2.** Average Density-Janka Hardness Values and Increase in Density

Group	Pressure (MPa)	Temperature (°C)	Duration (min)	Average Density (kg/m <sup>3</sup> )	Janka Hardness (kgf/cm <sup>2</sup> ) (N/mm <sup>2</sup> )	Increase in Density (%)*
Control	-	-	-	460	193,29 (18,95)	-
A	5	120	60	470	230,11 (22,56)	2
B	7	120	60	660	274,93 (26,96)	44
C	5	150	60	580	269,96 (26,47)	26
D	7	150	60	830	382,30 (37,49)	80

\* The values except for increase in density were found by Unsal and Candan (2008).  
 Increase in density (%) = [(Average density in Group X - Average density in Control Group) / Average density in Control Group]\*100.

## CONCLUSIONS

The influences of varying temperature (120°C and 150°C) and press pressure (5 MPa and 7 MPa) on the anatomical structure of thermally compressed solid-wood panels were investigated. Microscopic investigations showed that the deformations were not uniform throughout a growth ring, and the highest deformation occurred in earlywood regions of all growth rings for each process condition. The results showed that the same pressure level has much more effect in the wood deformation at higher temperatures.

This research indicated that there are significant interactions between process conditions and anatomical structure of wood. The wood exhibited different behavior in almost all process conditions, and the process conditions showed a different effect related to anatomical structure of wood, as in Group D (150°C-7 MPa). Sub-groups D<sub>1</sub> and D<sub>2</sub> behaved quite differently from each other. Sub-group D<sub>2</sub> showed no cell collapse in the earlywood region when compared to the sub-group D<sub>1</sub>. This was attributed to the principle that a homogenous structure in growth rings with uniform widths in earlywood and latewood regions has a strong effect on prevention of cell collapse.

Determination of changes in anatomical structure of wood is important for the development of a new product by means of using wood modification methods. Changes in the anatomical structure should not limit the use of modified wood in the standard industrial applications. In this context, applying a modification method on different wood species is not enough to clarify its success. It should be applied on the same wood species, which have different anatomical structures, and the results should be considered comparatively.

## ACKNOWLEDGMENTS

We would like to thank Incekara Holding for technical support for the Hitachi Tabletop Microscope TM-1000 (SEM) investigations.

## REFERENCES CITED

- Alexiou, P. N. (1994). "Elastic properties of *Eucalyptus pilularis* Sm. perpendicular to the grain," *Holzforschung* 48, 55-60.
- Ando, K., and Onda, H. (1999). "Mechanism for deformation of wood as a honeycomb structure II: First buckling mechanism of cell walls under radial compression using the generalized cell model," *Journal of Wood Science* 45(3), 250-253.
- Awoyemi, L., and Jones, I.P. (2010). "Anatomical explanations for the changes in properties of western red cedar (*Thuja plicata*) wood during heat treatment," *Wood Science and Technology* DOI 10.1007/s000226-010-0315-9.
- Blomberg, J., Persson, B., and Blomberg, A. (2005). "Effects of semi-isostatic densification of wood on the variation in strength properties with density," *Wood Science and Technology* 39, 339-350.
- Bodig, J. (1965). "The effect of anatomy on the initial stress-strain relationship in transverse compression," *Forest Products Journal* 15(5), 197-202.
- Bodig, J., and Jayne, B. A. (1982). *The Mechanics of Wood and Wood Composites*, Van Nostrand Reinhold Co.Inc., New York, NY.
- Boonstra, M. J., Rijdsdijk, J. F., Sander, C., Kegel, E., Tjeerdsma, B., Militz, H., Acker van, J., and Stevens, M. (2006). "Microstructural and physical aspects of heat treated wood. Part 1. Softwoods," *Maderas. Ciencia y Tecnologia* 8(3), 193-208.
- Burgert, I., Bernasconi, A., Niklas, K.J., and Eckstein, D. (2001). "The influence of rays on the transverse elastic anisotropy in green wood of deciduous trees," *Holzforschung* 55(5), 449-454.
- Dinwoodie, J. M. (1965). "The relationship between fibre morphology and paper properties," *Tappi Journal* 48(8), 440-447.
- Dinwoodie, J. M. (2000). *Timber. Its Nature and Behaviour*, BRE, London & New York.
- Easterling, K. E., Harryson, R., Gibson, L. J., and Ashby, M. F. (1982). "On the mechanics of balsa and other woods," *Proceedings of Royal Society London A* 383, 31-41.
- Fengel, D., and Wegener, G. (1989). *Wood Chemistry Ultrastructure Reactions*, Walter De Gruyter.
- Gong, M., Nakatani, M., Yang, Y., and Afzal, M.T. (2006). "Maximum compression ratios of softwoods produced in Eastern Canada," In: *Proceeding of 9<sup>th</sup> World Conference on Timber Engineering*, Portland, Oregon, August, ([www.ewpa.com/Archive/2006/aug/Paper\\_306pdf](http://www.ewpa.com/Archive/2006/aug/Paper_306pdf)).
- Hill, C. (2006). *Wood Modification, Chemical, Thermal and Other Processes*, Wiley, West Sussex.

- Irle, M., and Known, J. H. (2001). "Visualisation of cell wall collapse caused by the hot-pressing of wood particles," *In Proceedings of the Fifth European Panel Products Symposium*, Liandudno, Wales, United Kingdom.
- Kennedy, R. W. (1968). "Wood in transverse compression," *Forest Products Journal* 18(3), 36-40.
- Kubojima, Y., Oktani, T., and Yoshihara, H. (2003). "Effect of shear deflection on bending properties of compressed wood," *Wood and Fiber Science* 36, 210-215.
- Kunesh, R. H. (1961). "The inelastic behavior of wood: A new concept for improved panel forming process," *Forest Products Journal* 11, 395-406.
- Kunesh, R. H. (1968). "Strength and elastic properties of wood in transverse compression," *Forest Products Journal* 18, 36-40.
- Kutnar, A., and Šernek, M. (2007). "Densification of wood," *Zbornik Gozdarstva in Lesarstva* 82, 53-62.
- Müller, U., Gindl, W., and Teischinger, A. (2003). "Effects of cell anatomy on the plastic and elastic behaviour of different wood species loaded perpendicular to grain," *IAWA Journal* 24(2), 117-128.
- Nairn, J.A. (2006). "Numerical simulations of transverse compression and densification in wood," *Wood and Fiber Science* 38(4), 576-591.
- Navi, P., and Girardet, F. (2000). "Effects of thermo-hydro-mechanical treatment on the structure and properties of wood," *Holzforschung* 54, 287-293.
- Persson, M. S., Johansson, D., and Morén, T. (2006). "Heat treatment of solid wood: Effects on absorption, strength and color," Doctoral Thesis Paper V, "Effect of heat treatment on the microstructure of pine, spruce and birch and the influence on capillary absorption," Luleå University of Technology, LTU Skellefteå, Division of Wood Physics.
- Stefansson, F. (1995). "Mechanical properties of wood at microstructure level," *Report TVSM-5057*, Lund Institute of Technology, Lund, Sweden.
- Tabarsa, T. (1995). "The Effects of transverse compression and press temperature on wood response during hot-pressing," M.Sc., Thesis, The University of New Brunswick, Canada.
- Tabarsa, T., and Chui, Y. H. (1999). "Microscopic observation of wood behaviour in radial compressing," *In Proceedings of the Fourth International Conference on the Development of Wood Science, Wood Technology and Forestry*, Chilterns University College, Buckinghamshire, England.
- Tabarsa, T., and Chui, Y. H. (2000). "Stress-strain response of wood under radial compression. Part I. Test method and influences of cellular properties," *Wood and Fiber Science* 32, 144-152.
- Tabarsa, T., and Chui, Y. H. (2001). "Characterizing microscopic behaviour of wood under transverse compression. Part II. Effect of species and loading direction," *Wood and Fiber Science* 33, 223-232.
- Terziev, N., and Daniel, G. (2002). "Industrial kiln drying and its effect on microstructure, impregnation and properties of Scots pine timber impregnated for above ground use. Part 2. Effect of drying on microstructure and some mechanical properties of Scots pine wood," *Holzforschung* 56(4), 434-439.

- Unsal, O., and Candan, Z. (2007). "Effects of press pressure and temperature on the moisture content, vertical density profile and janka hardness of pine wood panels," In: *Proceedings of 10<sup>th</sup> International IUFRO Division-5, Wood Drying Conference, Orono, Maine, USA*, August 26-30.
- Unsal, O., and Candan, Z. (2008). "Moisture content, vertical density profile and janka hardness of thermally compressed pine wood panels as a function of pres pressure and temperature," *Drying Technology* 26(9), 1165-1169.
- Unsal, O., Kartal, S. N., Candan, Z., Arango, R. A., Clausen, C. A., and Green III, F. (2009). "Decay and termite resistance, water absorption and swelling of thermally compressed wood panels," *International Biodeterioration & Biodegradation* 63, 548-552.
- Walther, T. (2003). "The influence of moisture content and grain orientation on the compressibility and recovery of wood particles," Degree of Diplom-Holzwirt, Universität Hamburg, Ordinariat für Holztechnologie.
- Wang, J., and Cooper, P. A. (2005a). "Vertical density profiles in thermally compressed balsam fir wood," *Forest Products Journal* 55, 65-68.
- Wang, J. Y., and Cooper, P. A. (2005b). "Effect of grain orientation and surface wetting on vertical density profiles of thermally compressed fir and spruce," *Holz als Roh- und Werkstoff* 63, 397-402.
- Welzbacher, C. R., Wehsener, J., Rapp, A. O., and Haller, P. (2008). "Thermo-mechanical densification combined with thermal modification of Norway spruce (*Picea abies* Karst) in industrial scale – dimensional stability and durability aspects," *Holz als Roh- und Werkstoff* 66, 39-49.
- Wolcott, M. P., Kamke, F. A., and Dillard, D. A. (1994). "Fundamental aspects of wood deformation pertaining to manufacture of wood-base composites," *Wood and Fiber Science* 26(4), 496-511.
- Yoshihara, H., and Tsunematsu, S. (2007). "Bending and shear properties of compressed Sitka spruce," *Wood Science and Technology* 41, 117-131.

Article submitted: August 7, 2010; Peer review completed: September 14, 2010; Revised version received and accepted: October 21, 2010; Published: October 25, 2010.